

## Measurement of the $^{242}\text{Pu}(n,\gamma)$ cross section from thermal to 500 keV at the Budapest research reactor and CERN n\_TOF-EAR1 facilities

J. Lerendegui-Marco<sup>1,\*</sup>, C. Guerrero<sup>1,2</sup>, E. Mendoza<sup>3</sup>, J. M. Quesada<sup>1</sup>, K. Eberhardt<sup>4</sup>, A. Junghans<sup>5</sup>, M. Kr̄t̄icka<sup>6</sup>, T. Belgya<sup>7</sup>, B. Maróti<sup>7</sup>, O. Aberle<sup>8</sup>, J. Andrzejewski<sup>9</sup>, L. Audouin<sup>10</sup>, V. Bécares<sup>3</sup>, M. Bacak<sup>11</sup>, J. Balibrea<sup>3</sup>, M. Barbagallo<sup>12</sup>, S. Barros<sup>13</sup>, F. Bečvář<sup>6</sup>, C. Beinrucker<sup>14</sup>, E. Berthoumieux<sup>15</sup>, J. Billowes<sup>16</sup>, D. Bosnar<sup>17</sup>, M. Brugger<sup>8</sup>, M. Caamaño<sup>18</sup>, F. Calviño<sup>19</sup>, M. Calviani<sup>8</sup>, D. Cano-Ott<sup>3</sup>, R. Cardella<sup>8</sup>, A. Casanovas<sup>19</sup>, D. M. Castelluccio<sup>20,21</sup>, F. Cerutti<sup>8</sup>, Y. H. Chen<sup>10</sup>, E. Chiaveri<sup>8</sup>, N. Colonna<sup>12</sup>, G. Cortés<sup>19</sup>, M. A. Cortés-Giraldo<sup>1</sup>, L. Cosentino<sup>22</sup>, L. A. Damone<sup>12,23</sup>, M. Diakaki<sup>15</sup>, C. Domingo-Pardo<sup>24</sup>, R. Dressler<sup>25</sup>, E. Dupont<sup>15</sup>, I. Durán<sup>18</sup>, B. Fernández-Domínguez<sup>18</sup>, A. Ferrari<sup>8</sup>, P. Ferreira<sup>13</sup>, P. Finocchiaro<sup>22</sup>, V. Furman<sup>26</sup>, K. Göbel<sup>14</sup>, A. R. García<sup>3</sup>, A. Gawlik<sup>9</sup>, T. Glodariu<sup>†27</sup>, I. F. Gonçalves<sup>13</sup>, E. González-Romero<sup>3</sup>, A. Goverdovski<sup>28</sup>, E. Griesmayer<sup>11</sup>, F. Gunsing<sup>15,8</sup>, H. Harada<sup>29</sup>, T. Heftrich<sup>14</sup>, S. Heinitz<sup>25</sup>, J. Heyse<sup>30</sup>, D. G. Jenkins<sup>31</sup>, E. Jericha<sup>11</sup>, F. Käppeler<sup>32</sup>, Y. Kadi<sup>8</sup>, T. Katabuchi<sup>33</sup>, P. Kavrigin<sup>11</sup>, V. Ketlerov<sup>28</sup>, V. Khryachkov<sup>28</sup>, A. Kimura<sup>29</sup>, N. Kivel<sup>25</sup>, I. Knapova<sup>6</sup>, M. Kokkoris<sup>34</sup>, E. Leal-Cidoncha<sup>18</sup>, C. Lederer<sup>35</sup>, H. Leeb<sup>11</sup>, S. Lo Meo<sup>20,21</sup>, S. J. Lonsdale<sup>35</sup>, R. Losito<sup>8</sup>, D. Macina<sup>8</sup>, J. Marganiec<sup>9</sup>, T. Martínez<sup>3</sup>, C. Massimi<sup>21,36</sup>, P. Mastinu<sup>37</sup>, M. Mastroarco<sup>12</sup>, F. Matteucci<sup>38,39</sup>, E. A. Maugeri<sup>25</sup>, A. Mengoni<sup>20</sup>, P. M. Milazzo<sup>38</sup>, F. Mingrone<sup>21</sup>, M. Mirea<sup>27</sup>, S. Montesano<sup>8</sup>, A. Musumarra<sup>22,40</sup>, R. Nolte<sup>41</sup>, A. Oprea<sup>27</sup>, N. Patronis<sup>42</sup>, A. Pavlik<sup>43</sup>, J. Perkowski<sup>9</sup>, J. I. Porras<sup>8,44</sup>, J. Praena<sup>1,44</sup>, K. Rajeev<sup>45</sup>, T. Rauscher<sup>46,47</sup>, R. Reifarh<sup>14</sup>, A. Riego-Perez<sup>19</sup>, P. C. Rout<sup>45</sup>, C. Rubbia<sup>8</sup>, J. A. Ryan<sup>16</sup>, M. Sabaté-Gilarte<sup>8,1</sup>, A. Saxena<sup>45</sup>, P. Schillebeeckx<sup>30</sup>, S. Schmidt<sup>14</sup>, D. Schumann<sup>25</sup>, P. Sedyshev<sup>26</sup>, A. G. Smith<sup>16</sup>, A. Stamatopoulos<sup>34</sup>, G. Tagliente<sup>12</sup>, J. L. Tain<sup>24</sup>, A. Tarifeño-Saldivia<sup>24</sup>, L. Tassan-Got<sup>10</sup>, A. Tsinganis<sup>34</sup>, S. Valenta<sup>6</sup>, G. Vannini<sup>21,36</sup>, V. Variale<sup>12</sup>, P. Vaz<sup>13</sup>, A. Ventura<sup>21</sup>, D. Vescovi<sup>12,48</sup>, V. Vlachoudis<sup>8</sup>, R. Vlastou<sup>34</sup>, A. Wallner<sup>49</sup>, S. Warren<sup>16</sup>, M. Weigand<sup>14</sup>, C. Weiss<sup>8,6</sup>, C. Wolf<sup>14</sup>, P. J. Woods<sup>35</sup>, T. Wright<sup>16</sup>, P. Žugec<sup>17,8</sup>, and the n\_TOF Collaboration

<sup>1</sup>Dpto. Física Atómica, Molecular y Nuclear, Universidad de Sevilla, Sevilla, Spain

<sup>2</sup>Centro Nacional de Aceleradores(CNA), Seville, Spain

<sup>3</sup>Centro de Investigaciones Energéticas Medioambientales y Tecnológicas (CIEMAT), Madrid, Spain

<sup>4</sup>Johannes Gutenberg Universität Mainz, Mainz, Germany

<sup>5</sup>Helmholtz-Zentrum Dresden-Rossendorf, Dresden, Germany

<sup>6</sup>Charles University, Prague, Czech Republic

<sup>7</sup>Nuclear Analysis and Radiography Department, Hungarian Academy of Sciences, Budapest, Hungary

<sup>8</sup>European Organization for Nuclear Research (CERN), Switzerland

<sup>9</sup>University of Lodz, Poland

<sup>10</sup>Institut de Physique Nucléaire, CNRS-IN2P3, Univ. Paris-Sud, Université Paris-Saclay, F-91406 Orsay Cedex, France

<sup>11</sup>Technische Universität Wien, Austria

<sup>12</sup>Istituto Nazionale di Fisica Nucleare, Sezione di Bari, Italy

<sup>13</sup>Instituto Superior Técnico, Lisbon, Portugal

<sup>14</sup>Goethe University Frankfurt, Germany

<sup>15</sup>CEA Irfu, Université Paris-Saclay, F-91191 Gif-sur-Yvette, France

<sup>16</sup>University of Manchester, United Kingdom

<sup>17</sup>Department of Physics, Faculty of Science, University of Zagreb, Zagreb, Croatia

<sup>18</sup>University of Santiago de Compostela, Spain

<sup>19</sup>Universitat Politècnica de Catalunya, Spain

<sup>20</sup>Agenzia nazionale per le nuove tecnologie (ENEA), Bologna, Italy

<sup>21</sup>Istituto Nazionale di Fisica Nucleare, Sezione di Bologna, Italy

<sup>22</sup>INFN Laboratori Nazionali del Sud, Catania, Italy

<sup>23</sup>Dipartimento di Fisica, Università degli Studi di Bari, Italy

<sup>24</sup>Instituto de Física Corpuscular, CSIC - Universidad de Valencia, Spain

<sup>25</sup>Paul Scherrer Institut (PSI), Villigen, Switzerland

<sup>26</sup>Joint Institute for Nuclear Research (JINR), Dubna, Russia

<sup>27</sup>Horia Hulubei National Institute of Physics and Nuclear Engineering, Romania

<sup>28</sup>Institute of Physics and Power Engineering (IPPE), Obninsk, Russia

<sup>29</sup>Japan Atomic Energy Agency (JAEA), Tokai-mura, Japan

<sup>30</sup>European Commission, Joint Research Centre, Geel, Retieseweg 111, B-2440 Geel, Belgium

<sup>31</sup>University of York, United Kingdom

- <sup>32</sup>Karlsruhe Institute of Technology, Campus North, IKP, 76021 Karlsruhe, Germany
- <sup>33</sup>Tokyo Institute of Technology, Japan
- <sup>34</sup>National Technical University of Athens, Greece
- <sup>35</sup>School of Physics and Astronomy, University of Edinburgh, United Kingdom
- <sup>36</sup>Dipartimento di Fisica e Astronomia, Università di Bologna, Italy
- <sup>37</sup>Istituto Nazionale di Fisica Nucleare, Sezione di Legnaro, Italy
- <sup>38</sup>Istituto Nazionale di Fisica Nucleare, Sezione di Trieste, Italy
- <sup>39</sup>Dipartimento di Astronomia, Università di Trieste, Italy
- <sup>40</sup>Dipartimento di Fisica e Astronomia, Università di Catania, Italy
- <sup>41</sup>Physikalisch-Technische Bundesanstalt (PTB), Bundesallee 100, 38116 Braunschweig, Germany
- <sup>42</sup>University of Ioannina, Greece
- <sup>43</sup>University of Vienna, Faculty of Physics, Vienna, Austria
- <sup>44</sup>University of Granada, Spain
- <sup>45</sup>Bhabha Atomic Research Centre (BARC), India
- <sup>46</sup>Centre for Astrophysics Research, University of Hertfordshire, United Kingdom
- <sup>47</sup>Department of Physics, University of Basel, Switzerland
- <sup>48</sup>Istituto Nazionale di Fisica Nucleare, Sezione di Perugia, Italy
- <sup>49</sup>Australian National University, Canberra, Australia

**Abstract.** The design and operation of innovative nuclear systems requires a better knowledge of the capture and fission cross sections of the Pu isotopes. For the case of capture on  $^{242}\text{Pu}$ , a reduction of the uncertainty in the fast region down to 8-12% is required. Moreover, aiming at improving the evaluation of the fast energy range in terms of average parameters, the OECD NEA *High Priority Request List* (HPRL) requests high-resolution capture measurements with improved accuracy below 2 keV. The current uncertainties also affect the thermal point, where previous experiments deviate from each other by 20%. A fruitful collaboration between JGU Mainz and HZ Dresden-Rossendorf within the EC CHANDA project resulted in a  $^{242}\text{Pu}$  sample consisting of a stack of seven fission-like targets making a total of 95(4) mg of  $^{242}\text{Pu}$  electrodeposited on thin (11.5  $\mu\text{m}$ ) aluminum backings. This contribution presents the results of a set of measurements of the  $^{242}\text{Pu}(n,\gamma)$  cross section from thermal to 500 keV combining different neutron beams and techniques. The thermal point was determined at the Budapest Research Reactor by means of Neutron Activation Analysis and Prompt Gamma Analysis, and the resolved (1 eV - 4 keV) and unresolved (1 - 500 keV) resonance regions were measured using a set of four Total Energy detectors at the CERN n\_TOF-EAR1.

## 1 Motivation for measuring $^{242}\text{Pu}(n,\gamma)$

The long-term sustainability of nuclear energy requires to the use innovative nuclear systems like the Generation-IV reactors and Accelerator-Driven Systems. Such systems, featuring fast neutron spectra, or using new fuel compositions, such as MOX, require an improved knowledge of the neutron cross sections.

Among the involved neutron cross sections that need to be improved in terms of accuracy, the NEA recommends in one of its reports that the capture cross section of  $^{242}\text{Pu}$  should be measured with an accuracy of 8-12% between 2 keV and 500 keV [1], corresponding to the unresolved resonance region (URR). Moreover, the PROFIL post-irradiation experiments indicated that JEFF-3.1(=JEFF-3.3) could be overestimating the  $^{242}\text{Pu}(n,\gamma)$  cross section in the URR by 14% [2]. This discrepancy requires a consistent evaluation of the fast region in terms of resonance parameters. For this reason, the NEA included in its HPRL [3] the need for high-resolution  $^{242}\text{Pu}(n,\gamma)$  measurements in its resonance region (RRR) between 0.5 eV and 2 keV. Last, the discrepancies in this cross section also affect the thermal point, for which the 20% spread of experimental values [4] leads to a deviation of 15% between the different evaluated libraries [5–7].

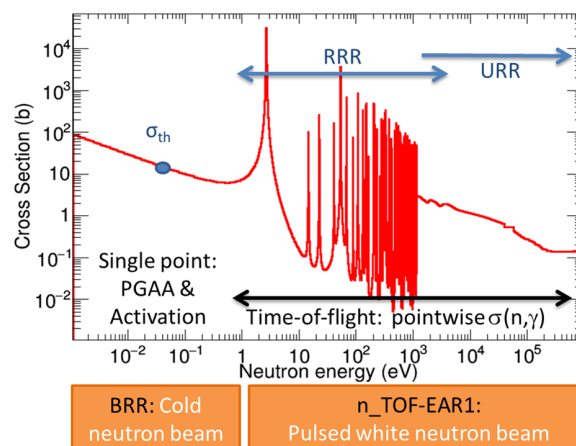


**Figure 1.**  $^{242}\text{Pu}(n,\gamma)$  cross section as a function of the neutron energy indicating the energy regions studied in this work using complementary neutron beams and different experimental technique.

## 2 Complementary beams and techniques with high quality $^{242}\text{Pu}$ targets

To provide a comprehensive measurement of this cross section in three neutron energy regions of interest (thermal, RRR and URR), different neutron beam facilities and experimental techniques have been used in this work (see

\*e-mail: jlerendegui@us.es

Figure 1). The thermal point was measured in the PGAA facility at the Budapest Research Reactor [8] and the resolved and unresolved resonance regions at n\_TOF facility at CERN [9].

A key factor for the success of the measurements has been the use of high quality  $^{242}\text{Pu}$  samples. A set of seven thin targets, each of 45 mm in diameter, were produced by electrodeposition of 95(4) mg of  $^{242}\text{Pu}$  enriched to 99.959% on thin (11.5  $\mu\text{m}$ ) aluminum backings. These *fission-like* targets feature a uniquely high ratio of actinide mass to neutron reaction rate on the target backings, hence improving the capture to background ratio with respect to other target designs [10].

### 3 Experiment at the Budapest Research Reactor

#### 3.1 Experimental facility and analysis methods

The experimental campaign was carried out at the Budapest Research Reactor (BRR). The neutron irradiations were performed at the PGAA facility, featuring a thermal-equivalent neutron flux of  $1.2 \cdot 10^8$  n/cm<sup>2</sup>/s and an average energy of 12 meV [8]. Four of the seven  $^{242}\text{Pu}$  targets available were assembled in two separate sandwiches that were used as samples.

One sample was irradiated together with a  $^{197}\text{Au}$  one and the  $^{242}\text{Pu}$  thermal cross section was determined by the activation technique measuring the  $\gamma$ -rays from the  $\beta$ -decay of  $^{243}\text{Pu}$  and  $^{198}\text{Au}$  in a low background measuring station equipped with a HPGe detector. During the irradiation of the second sample, the prompt  $\gamma$ -rays from the excited compound nucleus  $^{243}\text{Pu}$  were measured using a HPGe detector. A more detailed description of the experiment and analysis can be found in Ref. [11].

#### 3.2 Results of the $^{242}\text{Pu}$ thermal capture cross section

Previous measurements of the thermal capture cross section of  $^{242}\text{Pu}$  [4] deviate to each other by up to 20%, as shown in Figure 2. A recent measurement of the thermal point by Genreith et al. did not achieve enough accuracy to solve the previous discrepancies. In this work, the combination of different experimental methods has led to three compatible values for the thermal capture cross section of  $^{242}\text{Pu}$ :

- **Activation:** Capture cross section determined from the decay of the produced  $^{243}\text{Pu}$  nuclei relative to the  $^{197}\text{Au}$  thermal capture cross section. Consistent results were obtained for the four decay lines of  $^{243}\text{Pu}$  analyzed, which combined led to a value of 18.7(14) b.
- **PGAA single-line:** The partial  $\gamma$ -ray production cross section of the 287 keV prompt  $\gamma$ -ray was found to be 7.1(4) b, which leads to a thermal capture cross section of 17(3) b, using the absolute emission probability  $P_{287}=0.41(7)$  [12]). This method is limited by the large (17%) uncertainty of  $P_{287}$ .

- **PGAA unfolding method:** The capture cross section calculated using the energy-weighted sum rule applied to the full unfolded  $^{242}\text{Pu}(n,\gamma)$  spectrum (i.e. only full energy deposition) is 19.2(13) b. The description of this method can be found elsewhere [11]. In this approach, the absolute normalization to cross section is determined using the partial cross section for the 287 keV line mentioned above.

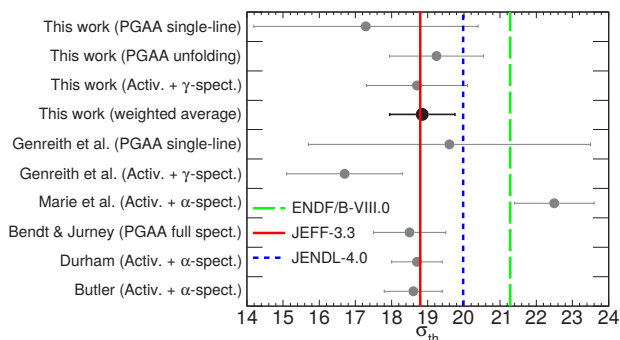


**Figure 2.** Thermal capture cross section values obtained in this work compared to previous experiments and the recommended values in the evaluated data libraries.

The weighted average of the results in this work, 18.9(9) b, improves the accuracy with respect to the latest trials, thus helping to solve the existing discrepancies. From the results in Figure 2, we conclude that our results are in good agreement with the previous measurements from Butler et al., Durham et al. and Bendt & Journey. On the other hand, the large value of Marie et al. can be now regarded as an outlier. The lowest value in Figure 2, the activation result by Genreith et al., yields 20.0(14) b after renormalization with the new intensity for the 84 keV decay line and becomes compatible with ours.

All the data sets in Figure 2 excluding the outlier of Marie et al. are compatible with 18.8(4) b, in very good agreement with our results. Comparing to the evaluations, this work supports JEFF-3.3 (18.79 b), while the ENDF-VIII.0 (21.28 b) evaluation, that gives significantly more weight to the result by Marie et al., and JENDL-4.0 (19.98 b) seem to overestimate the cross section by 13% and 6%, respectively.

### 4 Experiment at the CERN n\_TOF facility

#### 4.1 Experimental facility and analysis methods

The neutron capture cross section of  $^{242}\text{Pu}$  has been measured by means of the Time-of-Flight technique at the high-resolution n\_TOF facility (CERN), featuring one of the highest instantaneous neutron fluxes worldwide. The seven fission-like targets mentioned above were combined in a back-to-back stack [10]. This innovative target design has strongly reduced the background and the corrections associated to the  $\gamma$ -ray attenuation, neutron self-shielding and multiple scattering, among others. The experiment was carried out in the first experimental area (EAR1), located at 185 m from the spallation neutron source [13],

using an array of four  $C_6D_6$  scintillators to measure the prompt capture  $\gamma$ -rays of  $^{242}\text{Pu}$ . The Total Energy Detection method [14] was applied to determine the capture yield.

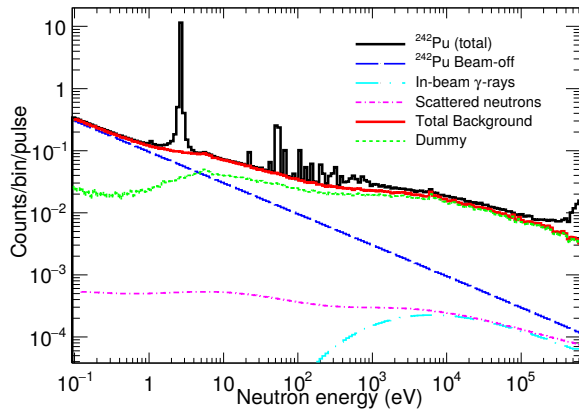


**Figure 3.** Total counting rate per pulse of  $^{242}\text{Pu}$  and contribution of the different background components. The counting rate in the URR ( $E_n > 1$  keV) is dominated by the beam related background (dummy) (see text for details).

The capture yield of  $^{242}\text{Pu}$  has been determined from 1 eV to 500 keV after a careful data reduction process described in detail in Refs. [15, 16]. One of the key points of the analysis is the assessment of the different background contributions, shown together with the total counts in Figure 3. The subtraction of the background, dominated by the dummy, was specially challenging in the URR, where it accounts for about 85% of the total measured counts. The  $^{242}\text{Pu}(n,\gamma)$  data have been reported up to 500 keV thanks to the correction for the  $(n, f)$  contribution using Monte Carlo simulations of the capture to fission efficiency ratio. A thorough minimization of the uncertainties was carried out, leading to a total systematic uncertainty in the capture yield which ranges from just 3% in the resonance region up to 12% in the URR.

#### 4.2 Resolved Resonance Region from 1 eV to 4 keV

The capture cross section of  $^{242}\text{Pu}$  has been extracted in the resonance region with a systematic uncertainty of only 5% (3% of the yield combined with 4% of the sample mass), which meets the requirements of the NEA-HPRL. A detailed description of the analysis of the RRR can be found in Ref. [15].

The R-Matrix analysis of the experimental capture yield (SAMMY) allows describing the cross section in terms of individual resonance parameters (RP). The good energy resolution of the facility and the large accumulated statistics have enabled the analysis of individual resonances up to 4 keV, while RP from previous capture measurements were only reported up to 1.3 keV (see Figure 4). The individual resonance parameters of 251 resonance have been extracted, 180 of which had never been

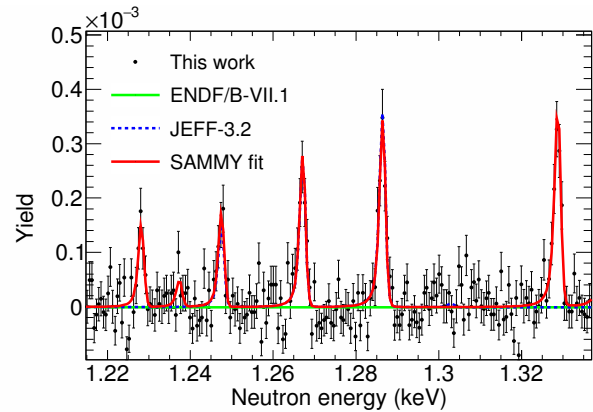


**Figure 4.** Capture yield measured at n\_TOF together with the SAMMY fit showing that our analysis includes resonances above the current limit of JEFF-3.2 (=JEFF-3.3).

reported before in any neutron capture measurement. Our analysis indicates a  $\sim 4\%$  higher capture cross section compared to JEFF-3.2 in terms of weighted average of resonance kernels ratio ( $\sim 6\%$  higher compared to the recent measurement at DANCE [20]).

The cross section at low energies is dominated by the 2.67 eV resonance, hence the relevance of obtaining accurate RP. A successful R-Matrix fit of this resonance required the inclusion of the Crystal Lattice Model (CLM) for the Doppler broadening as shown in Figure 5. The extracted resonance parameters are  $E_n=2.67625(3)$  eV,  $\Gamma_\gamma=25.4(6)$  meV and  $\Gamma_n=2.0965(19)$  meV, leading to a radiative kernel 4.2% larger than in ENDF/B-VIII.0 and JEFF-3.3 [5, 6], while DANCE reports a resonance integral larger than the value in ENDF/B-VIII.0 by 2.4% [20].

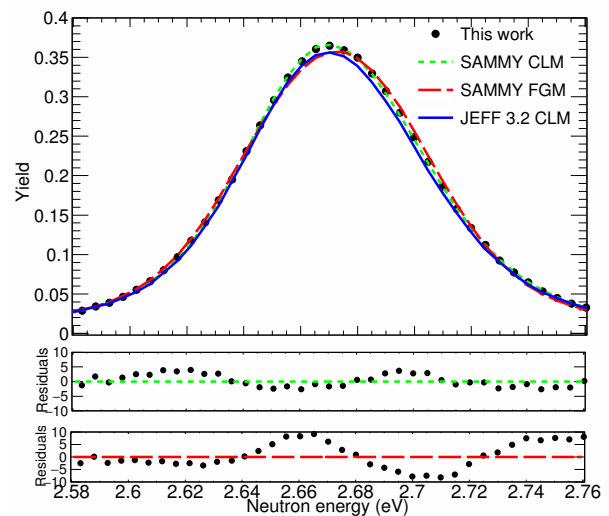


**Figure 5.** SAMMY fits and residuals of the first  $^{242}\text{Pu}$  resonance using Free Gas (FGM) and a Crystal Lattice (CLM) models for the Doppler broadening. The cross section obtained using the resonance parameters in JEFF-3.2 (=ENDF/B-VII.1) is shown as a reference.



Statistical model calculations, validated with different experimental observables, have allowed us to estimate the number of missed s-wave and visible p-wave resonances, based on the values of the reduced neutron widths. This statistical study has enabled to tag several resonances as p-wave candidates, ten of which are below 500 eV and are already considered as such in ENDF/B-VII.1.

The average resonance parameters have been calculated from the large set of analyzed s-wave resonances. From this analysis we obtained  $S_0=0.91(8)\cdot 10^{-4}$ , more accurate than in previous experiments and compatible with the values in the literature [15]. As for the average radiative width, the recommended value from our work is  $\langle\Gamma_\gamma\rangle=24.8(5)$  meV, significantly larger than most of the values in the literature and only compatible with JEFF-3.2 [5] and RIPL [17]. Last, the analysis of the observed number of s-wave resonances compared to the results of the statistical simulations mentioned before leads to a value of  $D_0=15.8(8)$  eV, consistent with JEFF-3.2, but significantly larger than the value in ENDF/B-VII.1 and RIPL.

### 4.3 Unresolved Resonance Region from 1 to 500 keV

The average capture cross section in the URR has been calculated from the capture yield measured at n\_TOF under the thin target approximation. The level of the systematic uncertainty, dominated by the background subtraction, ranges from 8 to 12%, meeting the target accuracy for the design for innovative nuclear systems in the energy range from 1 to 500 keV [1]. At higher energies, the data are not reported due to the large uncertainty associated to the correction for the contribution of the (*n,f*) channel. The reader is referred to Ref. [16] for the details of the analysis in the URR.

The measured cross section has been described in terms of average resonance parameters by means of a

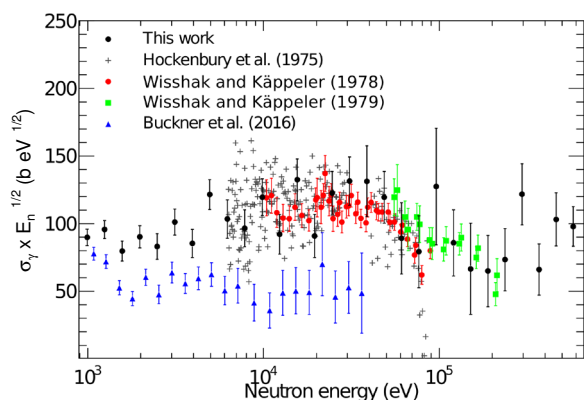


**Figure 6.** Capture cross section of  $^{242}\text{Pu}$  in the URR obtained in this work compared to the previous measurements available in EXFOR. The cross section has been multiplied by the square root of the neutron energy to remove the  $1/v$  dependence of the cross section.

Hauser-Feshbach calculation allowing width fluctuations with the SAMMY/FITACS code. The fitted values of  $S_0$  and  $\langle\Gamma_\gamma\rangle_0$  are consistent with those extracted from the RRR.

Our measurement is the first to provide  $^{242}\text{Pu}(n,\gamma)$  data in the full energy range of interest from 2 to 500 keV and shows a good agreement with the two previous measurements by Wisshak and Käppeler for neutron energies between 10 and 250 keV [18, 19], as shown in Figure 6. On the other hand, Figure 6 indicates that the strong reduction of the cross section suggested by the recent measurement in DANCE [20] is not confirmed by our results. The capture cross section in this work is, in average,  $\sim 10\text{-}14\%$  lower than JEFF-3.2 (=JEFF-3.3) in the energy range from 1 to 250 keV, in line with the interpretation of the PROFIL post-irradiation experiments [2].

## 5 Summary and conclusions

This work presents a series of measurements of the capture cross section of  $^{242}\text{Pu}$  from thermal to 500 keV using complementary neutron beams and different experimental techniques. The results presented in this manuscript were obtained from two different experiments carried out at the Budapest Research Reactor (BRR) and the n\_TOF-EAR1 facility at CERN using a set of high-quality  $^{242}\text{Pu}$  targets.

The new  $^{242}\text{Pu}(n,\gamma)$  data solve the existing discrepancies at thermal thanks to the improved accuracy. In the resonance region, the high resolution of n\_TOF-EAR1 has allowed to extract a large set of resonance parameters up to 4 keV. Last, this work provides the first data set in the URR covering the full energy range from 1 to 500 keV, and the results support the trend indicated by the PROFIL experiments to reduce the capture cross section in JEFF-3.2. In summary, the comprehensive measurement in this work shall contribute to a consistent re-evaluation of this cross section in the full energy range of interest.

## Acknowledgments

This measurement has received funding from the EC FP7 Programme under the projects NEUTANDALUS (Grant No. 334315) and CHANDA (Grant No. 605203), the Spanish Ministry of Economy and Competitiveness projects FPA2013-45083-P, FPA2014-53290-C2-2-P and FPA2016-77689-C2-1-R and the V Plan Propio de Investigación Programme from the University of Sevilla. Support from the German Federal Ministry for Education and Research (BMBF), contract number 03NUK13A, is gratefully acknowledged.

## References

- [1] M. Salvatores and R. Jacqmin, ISBN 978-92-64-99053-1, NEA/WPEC-26 (2008)
- [2] J. Tommasi and G. Noguere, Nucl. Sci. Eng. **160**, 232-241 (2008)
- [3] NEA Nuclear Data High Priority Request List, [www.oecd-nea.org/dbdata/hprl/](http://www.oecd-nea.org/dbdata/hprl/)

- [4] V.Semkova et al., Eur. Phys. J. Web Conf. **146** (2017)
- [5] A. Koning et al., J. Korean Phys. Soc. **59**, 1057 (2011)
- [6] M.B. Chadwick et al., *ENDF/B-VII.1*, Nucl. Data Sheets **112**, 2887 (2011)
- [7] K. Shibata et al., *JENDL-4.0: A New Library for Nuclear Science and Engineering*, J. Nucl. Sci. Technol. **48** 1 (2011)
- [8] T. Belgya et al., Proceedings of the European Research Infrastructures for Nuclear Data Applications (ERINDA) workshop, CERN, Geneva, 119–126 (2014)
- [9] E. Chiaveri et al., Proceedings of ND2019, Eur. Phys. J. Web Conf. (2019)
- [10] C. Guerrero et al., Nucl. Instrum. Methods A **925**, 87-91 (2019)
- [11] J. Lerendegui-Marco et al., Eur. Phys. J. A **55**, 63(2019)
- [12] C.D. Nesaraja and E.A. McCutchan, Nucl. Data Sheets **121**, 695 (2014)
- [13] C. Guerrero et al., Eur. Phys. J. A **49**, 27(2013)
- [14] R.L. Macklin, J.H. Gibbons, Phys. Rev. **159**, 1007 (1967)
- [15] J. Lerendegui-Marco et al., Phys. Rev. C **97**, 024605 (2018)
- [16] J. Lerendegui-Marco et al., Phys. Rev. C (submitted) (2019)
- [17] R. Capote et al., *Reference Input Parameter Library (RIPL-3)*, Nucl. Data Sheets **110**, Issue 12, 3107 (2009)
- [18] K. Wisshak and F. Käppeler, Nucl. Sci. Eng. **66**, 363 (1978)
- [19] K. Wisshak and F. Käppeler, Nucl. Sci. Eng. **69**, 39 (1979)
- [20] M.Q. Buckner et al., Phys. Rev. C **93**, 044613 (2016)